

The Implementation and Validation of a Bidirectional PWM Boost Rectifier Control Algorithm

Ionuț Deaconu*, Constantin Vlad Suru†, Mihăiță Lincă†, Cristina Alexandra Preda†

*Cummins Generator Technologies,

†Department of Electromechanics, Environment and Applied Informatics, University of Craiova
Craiova, Romania

vsuru@em.ucv.ro, mlinca@em.ucv.ro, apreda@em.ucv.ro

Abstract— The aim of this paper is the design and implementation of the control algorithm of a PWM boost rectifier capable to handle bidirectional energy flow. For this goal, the boost rectifier control loops must be tuned for the proper operation of absorbing active power from the power grid and transfer it to the dc load at constant output voltage, and also to give the rectifier the ability to generate back to the power grid the energy intake from the dc-link, using the dc-link capacitor as intermediary energy tank. It will be proved that the transition between rectifier operation and inverter operation is done automatically, without the intervention of the human operator or of a specially designed system. The correct implementation and tuning of the control algorithm was validated on a complete Matlab Simulink model which includes in detail all the sections of the rectifier system. The simulation and experimental results proved the correct answer of the tuned dc-link voltage controller and the overall operation of the system for a step changing active load. Because the boost rectifier control algorithm is similar to shunt active filters control algorithm, the indirect current control approach was adopted, which is the most suitable for this purpose.

Cuvinte cheie: *redresor PWM, algoritm de comandă, transfer bidirecțional de putere, reglaj în buclă închisă.*

Keywords: *PWM rectifier, control algorithm, bidirectional power flow, closed loop control.*

I. INTRODUCTION

Although the dc motor drive systems are less used nowadays, they are still used on a smaller scale and, moreover, the high power ac-dc conversion is applied on other applications. The most representative is the drive system with voltage and frequency converter and induction motor, because they are fed from the ac power grid.

The problems introduced to the power grid by the classical diode rectifiers are well known, and a way to mitigate the harmonic distortion is the use of PWM rectifiers. This is because the current absorbed by the rectifier from the power grid is sinusoidal, in phase with the voltage and with low harmonic content. This is because the boost PWM rectifier works like an inverter

which absorbs an imposed sinusoidal current from the grid in order to charge the dc-link capacitor. For this the inductive interface filter mounted between the power grid and the rectifier is mandatory.

A typical problem of both thyristor and buck PWM rectifiers is the unidirectional power flow, thus the incapacity of these rectifiers to recover the braking energy in (especially traction) drive systems [1-7].

This problem is overcome by the boost rectifier which can intrinsically sustain the bidirectional power flow: when the load absorbs power the transistor bridge works as rectifier and when the load produces power the transistor bridge works as an inverter.

Although, the boost rectifier has its disadvantages: it can only work in closed loop control and the output voltage cannot be less than the grid voltage amplitude (thus it can't be used directly for dc motor drive systems).

In this paper, the control algorithm of a closed loop boost rectifier is implemented in the Matlab Simulink environment, tested by simulation, and finally validated using the corresponding experimental setup.

After the introduction, in the second chapter of his paper a short presentation of the closed loop control algorithm is given - the design of the control algorithm is given in detail in the previous work of the authors [1][3-10]. The algorithm implementation in a comprehensive Simulink model is described in the third chapter and in the fourth chapter the simulation results are given. In the fifth chapter the experimental setup and the obtained experimental results are presented. Finally, the conclusions are drawn.

II. CLOSED LOOP CONTROL ALGORITHM

The boost PWM rectifier (Fig. 1) control algorithm is very similar with the shunt power active filter control algorithm, both in the control structure and in the working principle [8].

The difference between the two converters consists in the active power absorbed by the dc-link capacitor.

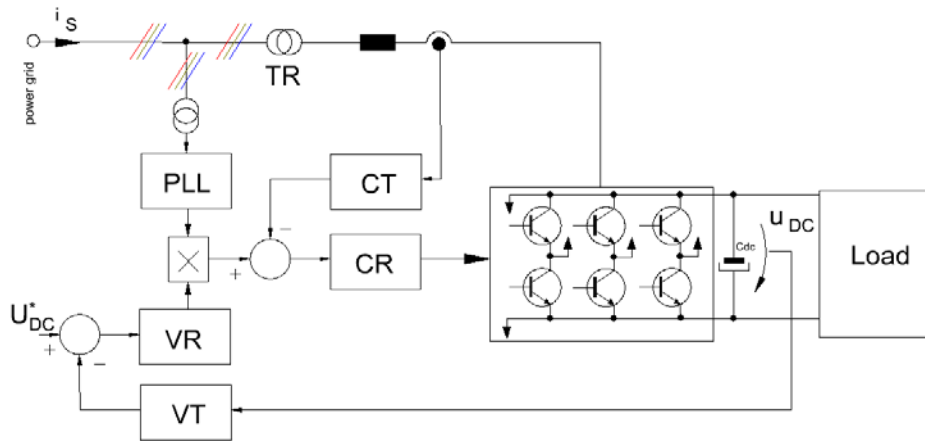


Fig. 1. The PWM boost rectifier block diagram.

The active filter dc-link capacitor (which is the compensating capacitor) absorbs in theory no active energy, it only changes reactive and distortion energy with the power grid and the nonlinear loads. The small amount of active power absorbed by the active filter from the power grid is used to cover the system losses. Therefore, the active filter power section is designed based on the rated apparent power of the nonlinear loads [1]. On the contrary, the PWM rectifier absorbs only active power, and in theory does not change non-active energy with the power grid.

This conducts to the following:

- If an active power is absorbed from the dc-link capacitor, its voltage tends to drop, therefore an active current is absorbed from the power grid to recharge the capacitor;
- If an active power is injected to the dc-link capacitor by the load (braking energy for example), its voltage tends to increase, and therefore an active current is injected to the power grid to discharge the capacitor.

Concluding, the boost PWM rectifier control algorithm is the same as for the shunt active filter (Fig. 2), therefore, the PI voltage regulator tuning procedure could be similar.

The output of the dc-link voltage controller is the power grid current amplitude which is positive when the rectifier load discharges the capacitor (the power grid current keeps the capacitor charged) and it is negative when the rectifier load charges the capacitor (and the power grid current discharges it) – Fig. 2.

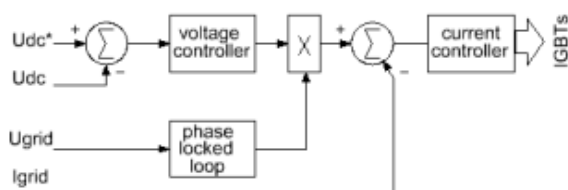


Fig. 2. The PWM boost rectifier control algorithm.

While the current controller is a simple hysteresis controller, the voltage controller is a proportional-integrative controller. For the tuning process of the latter, the transfer functions of the system components are used (Fig. 3) [1]:

- The partial transfer function of the power rectifier (considering the power transformer), from the rectifier control voltage to the power grid absorbed current, G_{Ri} :

$$G_{Ri} = \frac{I_s(s)}{U_{ci}(s)} = \frac{U_{dc-link} \cdot K_{TR}}{2R_k U_{rmax} (1 + T_k s)} = \frac{K_{Ai}}{1 + T_k \cdot s} \quad (1)$$

- The second partial transfer function of the power rectifier, from the power grid absorbed current to the dc-link capacitor voltage, G_{Ru} :

$$G_{Ru} = \frac{U_{dc-link}(s)}{I_s(s)} = \frac{\sqrt{3} \cdot U_{grid}}{C_{dc} \cdot U_{dc-link} \cdot s} = \frac{1}{K_{Au} \cdot s} \quad (2)$$

- The transfer function of the voltage controller, G_{vc} :

$$G_{vc} = K_{Pu} \cdot \left(1 + \frac{1}{T_{Iu} \cdot s} \right) = \frac{1 + \theta_{Iu} \cdot s}{\theta_u} \quad (3)$$

- The transfer function of the current transducer and of the voltage transducer, G_{Ti} , G_{Tu} :

$$G_{Ti} = \frac{K_{Ti}}{1 + T_{Ti} \cdot s}, \quad G_{Tu} = \frac{K_{Tu}}{1 + T_{Tu} \cdot s} \quad (4)$$

Because the current controller is a simple Three-Phase hysteresis controller, the transfer function of the current loop is unitary [1]. The hysteresis band was chosen 5% of the maximum current of 15 A, which is 0.75 A.

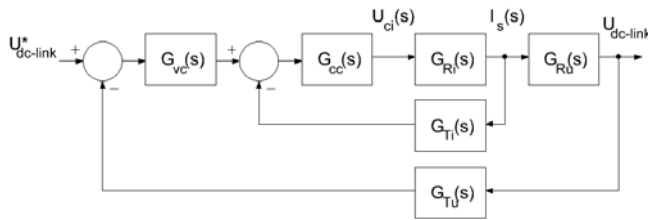


Fig. 3. The block diagram of the closed loop control algorithm.

The main parameters of the power section are [9-10]:

- Power grid phase voltage: 220 V;
- 1st order interface filter:
 - L = 0.634 mH;
- Power IGBTs:
 - V_{CES} = 1200 V, I_C = 300 A;
- DC Link capacitor:
 - C = 2200 μF;
- DC load:
 - I₁ = 15, I₂ = -15

Using the Symmetrical Optimum criterion, the tuning of the voltage controller led to the following results [1]:

$$K_{Pu} = \frac{\theta_{Iu}}{T_{Iu}} = 4.28, \quad T_{Iu} = \theta_u = 2.073 \cdot 10^{-6} \quad (5)$$

III. THE VIRTUAL IMPLEMENTATION OF THE PWM BOOST RECTIFIER

The PWM boost rectifier was virtually implemented in the Matlab Simulink environment (Fig. 4).

The power section which includes the power grid, the power transformer and power inverter, the interface filter, the dc-link capacitor and dc load was implemented using SimPowerSystems blocks, grouped in masked subsystems for an easier usage.

The dc load (Fig. 4) was simply implemented using a resistance (to impose the current) and a controlled voltage source (the dc load must be able to discharge and to charge the dc-link capacitor).

The boost rectifier Simulink model includes the control algorithm grouped in a masked subsystem (Fig. 5). This subsystem contains the implementation of the regulating loops in Fig. 3 to which some auxiliary blocs were added. The auxiliary blocks are necessary for the startup process of the boost rectifier, the synchronization to the power grid voltage (the voltage template), and also, for the reconstruction of Three-Phase voltages and currents measured by two transducers.

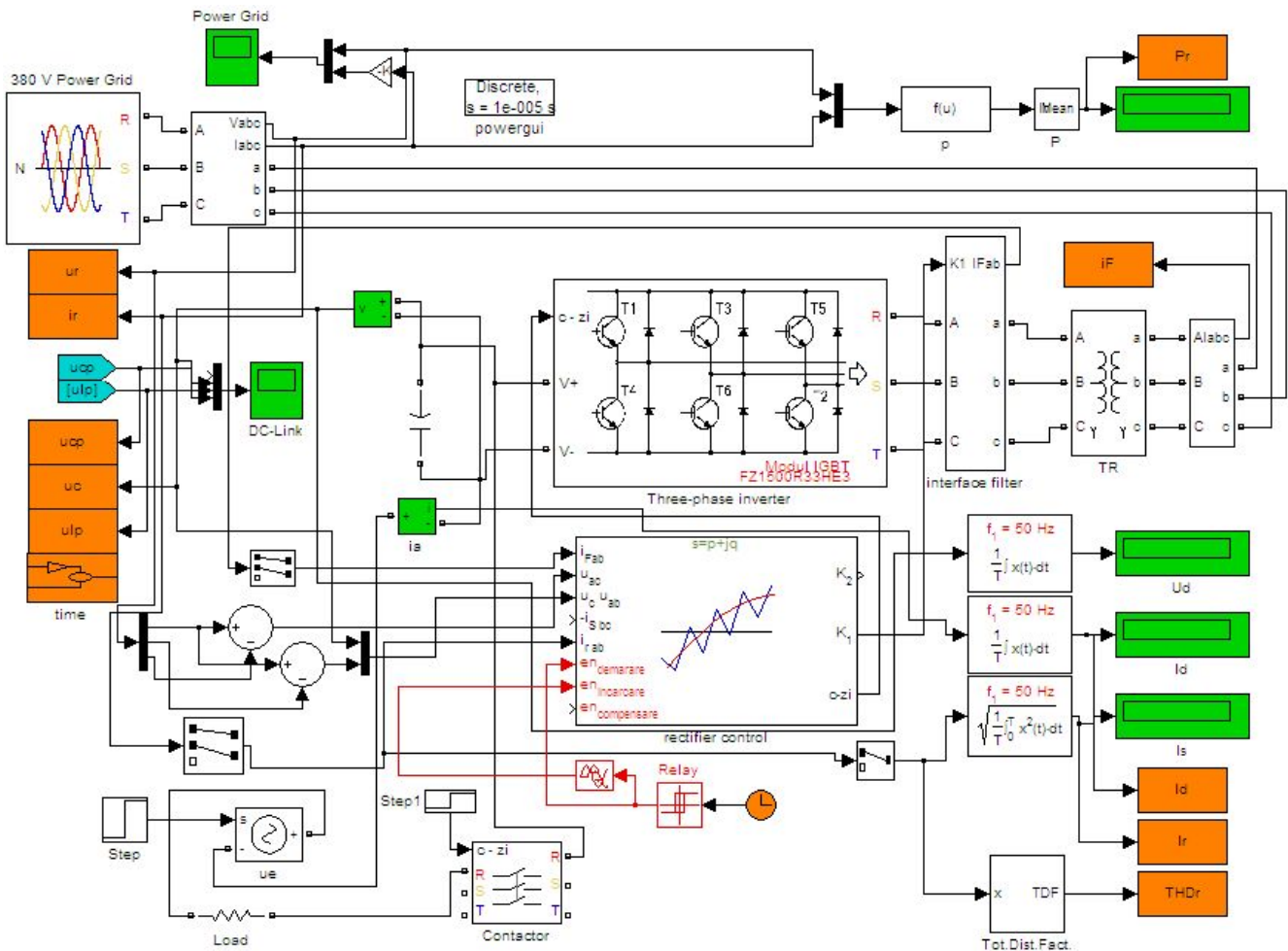


Fig. 4. The virtual implementation of the PWM Boost Rectifier system.

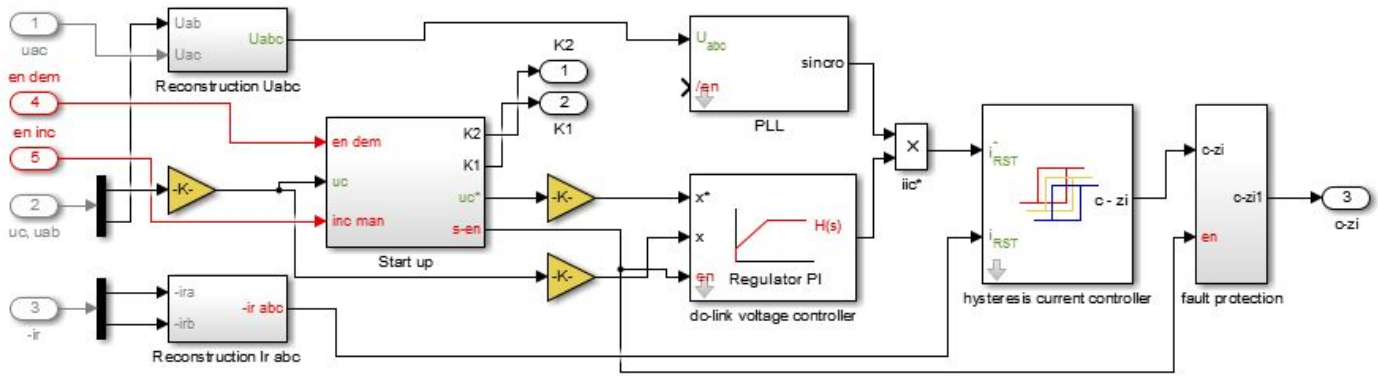


Fig. 5. The Boost PWM Rectifier control algorithm.

The start-up process is necessary, because the boost rectifier cannot start with the dc load connected [8]:

- The current limiting resistance can't sustain the load current;
- Considering the case when the load is at its rated value (34 A in the virtual implementation (Fig. 3)) the voltage regulator is at its saturation limit so there is no active current left to be absorbed from the power grid to charge the dc-link capacitor – if the load is smaller than its rated value, the capacitor can charge as faster as the load is smaller (assuming the fact that the rectifier had surpassed the resistive current limiting stage).

So the dc load is connected through a contactor after the initializing stage was completed (0.2 s – Fig. 3, Fig. 6).

The PLL (phase locked loop) gives the voltage template which is a three phase unitary amplitude sinusoidal signal in phase with the grid voltage [8]. The voltage template multiplied with the voltage regulator output gives the prescribed current [1][13].

IV. SIMULATION RESULTS

The boost rectifier system was investigated by simulation regarding both the dynamic and stationary operating regimes.

After the start-up process, the dc-load was connected to the dc-link. The with-load operation was investigated both in rectifier operation and inverter operation.

The dc-link voltage during the entire simulation time span is illustrated in Fig. 6. The voltage ripple is about 445 mV in rectifier operating mode ($t \in (0.2, 0.5)$) and about 293 mV in inverter operating mode ($t \in (0.5, 0.7)$), for an imposed output value of 220 V.

The closed loop charging of the dc-link capacitor lasts about 65 ms, although a small overshoot can be noted. The voltage overshoot is 5.29 V and the steady state operation is reached in 33.9 ms after the imposed voltage is 220V.

When $t = 0.2$ ms the output contactor is closed and the load is connected to the dc-link capacitor. The current drawn by the load from the dc-link is 14.97 A, and the capacitor voltage decrease is insignificant. The power grid current waveforms during this transitory regime are illustrated in Fig. 7. The current drawn by the load from the capacitor causes the voltage controller to impose an active current absorbed from the power grid of 5.59 A.

This gives an active power absorbed from the power grid of 3.66 kW and an output power of 3.3 kW so the global efficiency of the PWM boost rectifier in rectifier operation is 90.16%.

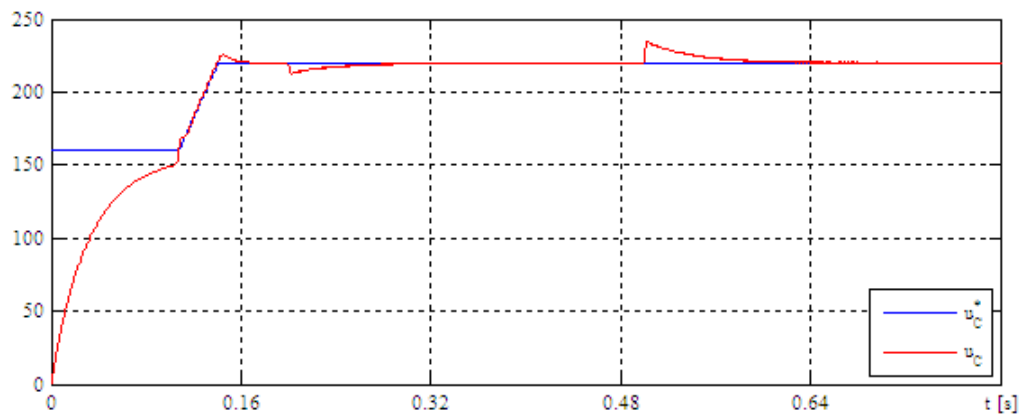


Fig. 6. The dc-link voltage during the entire simulation time span.

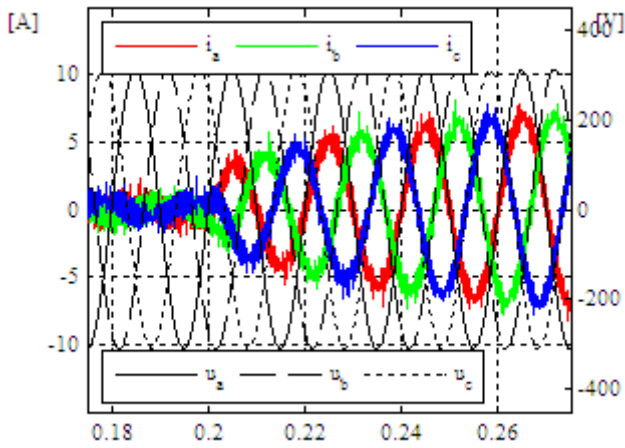


Fig. 7. The grid current of the PWM boost rectifier when the dc load is connected.

Regarding the dynamic response of the rectifier system, the dc-link voltage reaches steady-state after 142 ms. The initial voltage drop is 7.61 V and after reaching the steady-state regime, the dc-link capacitor average voltage is 219.93 V.

The power grid current waveforms in steady-state rectifier operation are illustrated in Fig. 8. The total harmonic distortion factor of these currents is 9.21%.

At $t = 0.5$ ms the dc-load changes its character and becomes regenerative (the generated voltage increases from 210 V to 230 V). The current generated by the load to the dc-link is -14.97 A, causing the capacitor voltage increase to about 22.03 V in static regime.

The power grid current waveforms during this transitory regime are illustrated in Fig. 9. This load causes the voltage controller to impose an active current injected to the power grid of 4.44 A.

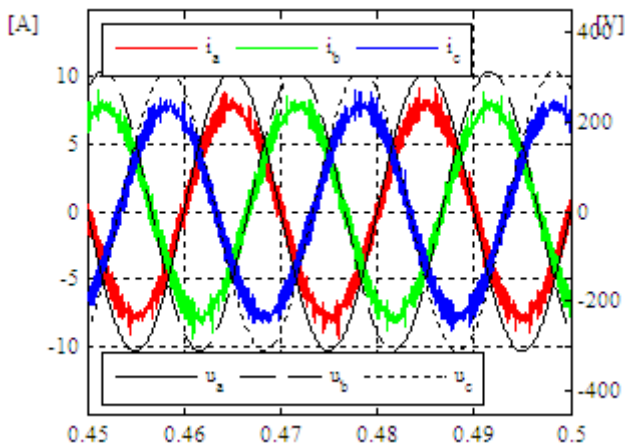


Fig. 8. The grid current of the PWM boost rectifier in steady-state rectifier operation.

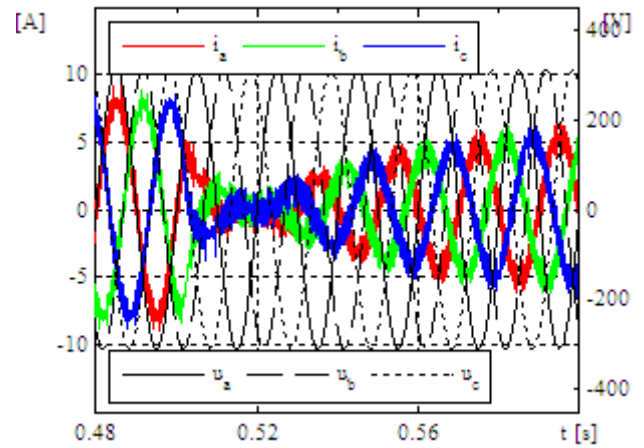


Fig. 9. The grid current of the PWM boost rectifier when the dc load becomes regenerative.

This gives an active power generated to the power grid of 2.90 kW for an input power of 3.28 kW so the global efficiency of the PWM boost rectifier in inverter operation is 88.41%.

Regarding the dynamic response of the rectifier system, the dc-link voltage reaches steady-state after 219.4 ms. The initial voltage increase is 15.49 V and after reaching the steady-state regime, the dc-link capacitor average voltage is 220.03 V.

The power grid current waveforms in steady-state inverter operation are illustrated in Fig. 10. The total harmonic distortion factor of these currents is 11.55%.

It results that the closed loop controlled PWM boost rectifier has good performances in both rectifier and energy recovery inverter operation, the transition between the two operating regimes being natural and fast. It can be noted that the efficiency is somewhat lower in recovery operation.

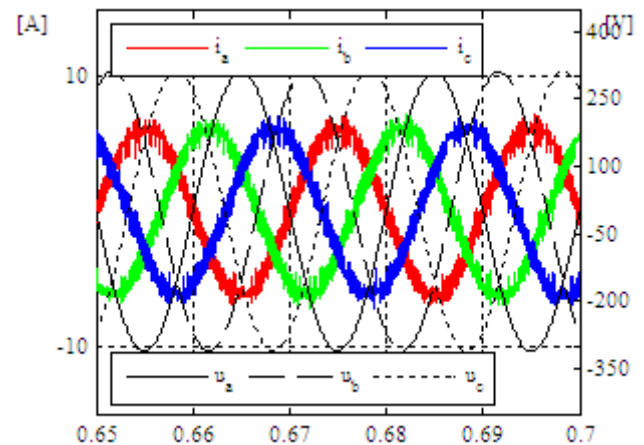


Fig. 10. The grid current of the PWM boost rectifier in steady-state inverter operation.

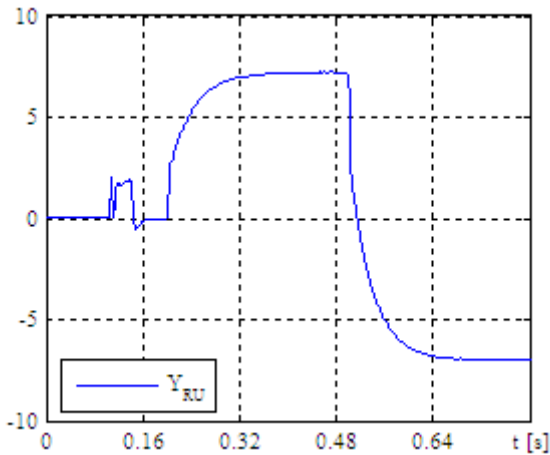


Fig. 11. The voltage controller output during the entire simulation time span.

The voltage controller performance affects both the input and the output.

At the input, the harmonic distortion of the grid currents in both rectifier and inverter modes are dependent on the voltage controller output (Fig. 11). Therefore, if the voltage controller is not tuned correctly, then in steady-state operation its output is not constant so the imposed grid current cannot be sinusoidal. For example, in Fig. 11 it can be noticed that for the above stated performances, the voltage controller output has no significant ripple.

If the voltage controller is not tuned correctly, then the boost rectifier doesn't absorb sufficient active power from the power grid, so the rectifier cannot sustain the imposed output voltage. Thus, in rectifier operation the voltage drops from the imposed voltage and in inverter operation the voltage increases. This also has effect on the rectifier efficiency, thus a poor voltage controller performance has a reduction effect on efficiency.

V. EXPERIMENTAL RESULTS

The results obtained by simulation were validated on an experimental PWM rectifier system consisting of:

- Three-phase Y- Δ transformer;
- 0.634 mH 1st order interface filter;
- Power inverter (300 A, 1200 V IGBTs);
- 2200 μ F dc-link capacitor;

The dc active load is a dc motor mechanically connected to a synchronous machine (Fig. 12). The latter is connected to the power grid and works:

- as generator when the dc motor absorbs power from the PWM rectifier and further on, from the power grid;
- as motor when the dc machine generates power to the PWM rectifier and further on, to the power grid.



Fig. 12. The active load of the boost PWM rectifier

The rated parameters of the dc machine are:

- $U_N = 220$ V;
- $I_N = 34$ A;
- $P_N = 6.2$ kW;
- $n_N = 1500$ rpm.

The rated parameters of the synchronous machine are:

- $U_{N1-1} = 400$ V;
- $I_N = 17.9$ A;
- $P_N = 6.2$ kW;
- $n_N = 1500$ rpm.

The PWM rectifier control section consists of a dSpace DS1103 control board, therefore the control algorithm of the rectifier implemented in the Simulink model in Fig. 4 was processed and compiled to the control board program memory (Fig. 13). So, there was no difference between the virtual system control algorithm and the experimental system one.

The signals from the power section are transmitted to the control algorithm by means of the DS1103 board ADCs and their corresponding RTI Simulink library blocks [15-16].

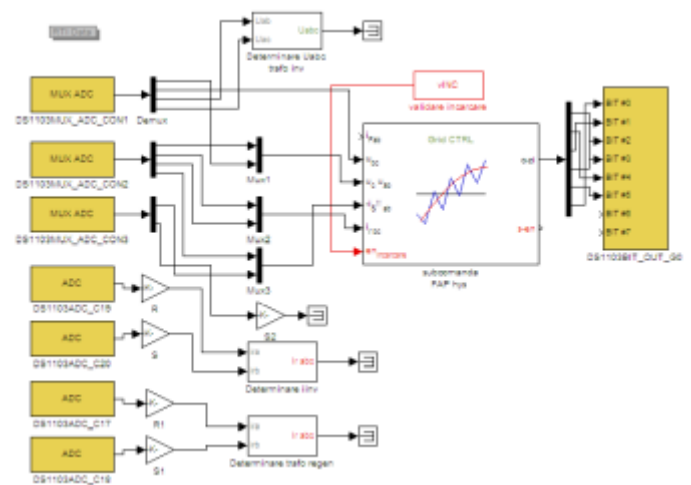


Fig. 13. The implementation of the boost PWM rectifier control algorithm for the dSpace DS1103 control board

For the first experiment, the boost rectifier was connected to the power grid and the dc-link capacitor was actively charged to the rated value of 220 V. Then, the dc machine was connected to the rectifier output (and the synchronous machine to the power grid), and by adjusting the rectifier output voltage as well as the dc machine field current, rectifier load current was adjusted to about 15 A (rectifier operation – the dc machine in motor operation).

The current absorbed from the power grid was measured using the experimental rectifier transducer system and for the analog to digital conversion the DS1103 ADCs were used [15-16]. Therefore, all the sampled signals were available as Matlab variables, the numerical analysis as well as the illustration of these signals being performed using the Matlab (Simulink) environment.

The mean current absorbed by the dc motor from the rectifier output, of about 15 A, imposed a grid current (illustrated in Fig. 14) with the RMS value of 6.29 A. The total harmonic distortion factor of the latter is 8.22%.

At the same time, the electrical power absorbed from the power grid by the rectifier system is 3.686 kW for an electrical power absorbed by the dc motor of 3.3 kW. This gives the system efficiency of 89.53%.

The power grid voltage and current was also measured with the Metrix Ox7042-M digital oscilloscope the screen capture being illustrated in Fig. 15.

In the second experiment, by adjusting the dc machine field current the synchronous machine entered motor operation while the dc machine entered generator operation (the rectifier imposed voltage was kept constant at 220 V).

The current generated to the power grid is illustrated in Fig. 16. The current absorbed by the rectifier from the DC machine was adjusted to give about the same RMS value of the grid current as the previous experiment.

It can be seen that in this case the current phase is opposite to the voltage phase meaning the rectifier works as an inverter.

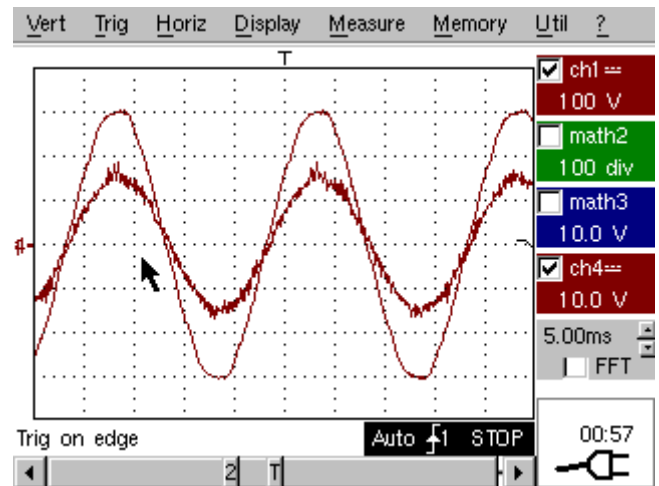


Fig. 15. The experimental grid current of the PWM boost rectifier in steady-state rectifier operation oscilografiated with the Metrix Ox7042-M digital oscilloscope.

Analyzing the grid current, it's RMS value is 6.28 A for a DC current absorbed from the DC machine of 19.5 A. This gives a electrical power absorbed from the generator of 4.29 kW and a recovered power to the grid of 3.73 kW. The rectifier system overall efficiency is 86.96%.

The total harmonic distortion factor of the grid current in inverter operating mode is 11.66%.

The power grid voltage and current for this experiment are illustrated in Fig. 17.

It must be mentioned that, the scaling difference between the oscillogram grid current (for both Fig. 15 and Fig. 17) and the corresponding current plotted in Matlab based on the data sampled by the DS1103 ADCs (in Fig. 14 and Fig. 16, accordingly) is due to the fact that the oscillogram grid current was taken using the rectifier system transducers so the current amplitude is relative and dependent on the current transducer V/A ratio.

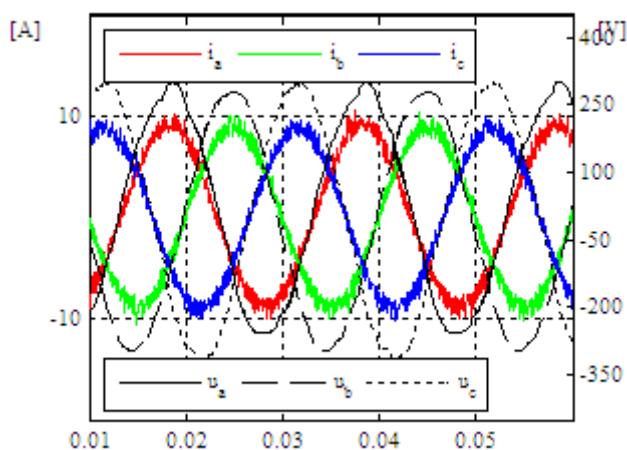


Fig. 14. The experimental grid current of the PWM boost rectifier in steady-state rectifier operation sampled by the DS1103 board and plotted in Matlab.

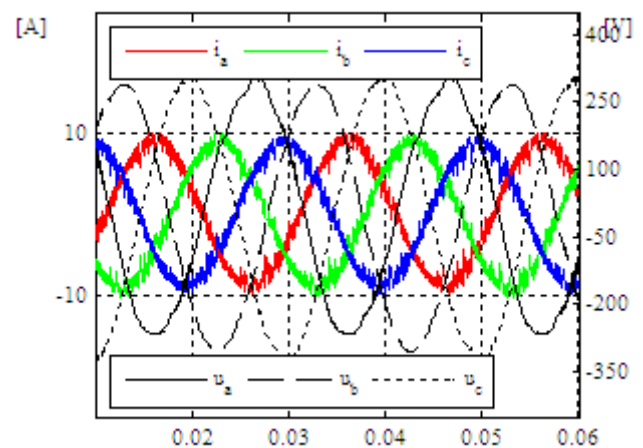


Fig. 16. The experimental grid current of the PWM boost rectifier in steady-state inverter operation sampled by the DS1103 board and plotted in Matlab.

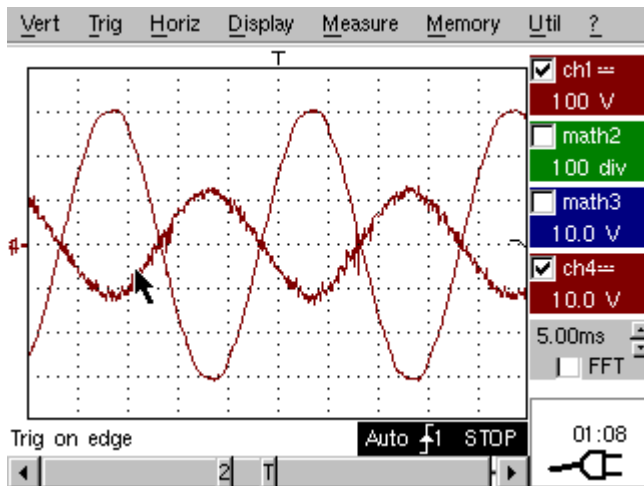


Fig. 17. The experimental grid current of the PWM boost rectifier in steady-state inverter operation oscilografated with the Metrix Ox7042-M digital oscilloscope.

VI. CONCLUSIONS

In this paper, the implementation of a control algorithm for a bidirectional PWM boost rectifier has been performed. The correct tuning and implementation was verified and validated both on a comprehensive Simulink model and on an experimental setup. The system operation was correct both in rectifier and inverter regimes, the transition from the rectifier to inverter operating mode and back being done naturally, without modification or different tuning of the control algorithm. Actually, the operating regime is not imposed by the rectifier control section but by the load. If the load absorbs power, the dc-link voltage decreases, imposing the rectifier mode and if the load gives power, the dc-link voltage increases imposing the inverter mode. The structure and rated values of the boost PWM rectifier Simulink model are related to the structure and rated values of the experimental setup. The obtained experimental results are related to the simulation results validating the correct implementation of the control algorithm. This algorithm can be used in high energetic performance rectifiers which can have the ability to compensate nonlinear AC loads due to its similitude to the active filters (both power section and control algorithm).

ACKNOWLEDGMENT

This work was performed through the program Partnerships in priority areas — PN II, conducted with the financial support of MEN – UEFISCDI, project no. PN-II-PT-PCCA-2013-4-0564 (42/01.07.2014).

Contribution of authors:

First author – 40%

First coauthor – 20%

Second coauthor – 20%

Third coauthor – 20%

Received on November 1, 2017

Editorial Approval on November 15, 2017

REFERENCES

- [1] A Bitoleanu, M Popescu, Active Filtering and regeneration System Dedicated to DC Active Traction Substations, The 18th National Conference on Electrical Drives, CNAE 2016, Acta Electrotechnica, Volume 57, Number 3-4, 2016, Special Issue, ISSN 2344-5637.
- [2] L He, J Xiong, H Ouyang, High-Performance Indirect Current Control Scheme for Railway Traction Four-Quadrant Converters, IEEE Trans. Ind. Electron., vol. 61, no. 12, pp. 6645-6654, December 2014.
- [3] M Popescu, A Bitoleanu, V Suru, Indirect current control in active DC railway traction substations, 2015 Intl Aegean Conference on Electrical Machines & Power Electronics (ACEMP), 2015 Intl Conference on Optimization of Electrical & Electronic Equipment (OPTIM) & 2015 Intl Symposium on Advanced Electromechanical Motion Systems (ELECTROMOTION), Electronic ISBN: 978-1-4673-7239-8, USB ISBN: 978-1-4673-7547-4, 2015, DOI: 10.1109/OPTIM.2015.7426954.
- [4] V Suru, M Popescu, I Deaconu, Study of Indirect Current Control Methods for Urban Traction Active DC Substations, Annals of the University of Craiova, Electrical Engineering series, No. 39, ISSN: 1842-4805, 2014, pp. 50-55.
- [5] V Suru, A Bitoleanu, M Linca, Indirect Current Control of a Filtering and Regeneration System used in DC Substations for Urban Traction, ATINER CONFERENCE PAPER SERIES No 2015-1562, 2015, 8-11 June 2015, pp. 1-6, ISSN: 2241-2891.
- [6] M Popescu, A Preda, V Suru, Synchronous Reference Frame Method Applied in the Indirect Current Control for Active DC Traction Substation, Athens: ATINER'S Conference Paper Series, No: TRA2015-1552, 2015, 8-11 June 2015, pp. 1-6, ISSN: 2241-2891.
- [7] A Bitoleanu, M Popescu, V Suru, Optimal Controllers Design in Indirect Current Control System of Active DC-Traction Substation, Conference: 17th IEEE International Power Electronics and Motion Control Conference (PEMC) Location: Varna, BULGARIA Date: SEP 25-28, 2016, 2016 Book Series: IEEE International Power Electronics and Motion Control Conference IPEMC Pages: 912-917, Published: 2016, ISBN:978-1-5090-1798-0.
- [8] CV Suru, M Linca, A Preda, E Subtirelu, Design and Analysis of the Compensating Capacitor Charging Algorithm for Active Filtering Systems, Conference: 17th IEEE International Power Electronics and Motion Control Conference (PEMC) Location: Varna, BULGARIA Date: SEP 25-28, 2016, Sponsor(s): IEEE Ind Elect Soc; IEEE Ind Applicat Soc; IEEE; Tech Univ Sofia; New Univ Lisbon, 2016 IEEE INTERNATIONAL POWER ELECTRONICS AND MOTION CONTROL CONFERENCE (PEMC) Book Series: IEEE International Power Electronics and Motion Control Conference IPEMC Pages: 889-896 Published: 2016, ISBN:978-1-5090-1798-0.
- [9] A Bitoleanu, M Popescu, D Marin, M Dobriceanu, LCL Interface Filter Design for Shunt Active Power Filters, 3rd International Symposium on Electrical Engineering and Energy Converters, September 24-25, 2009, Suceava.
- [10] CV Suru, A Bitoleanu, Design and Performances of Coupling Passive Filters in Three-Phase Shunt Active Power Filters, Analele Universitatii Din Craiova - Seria Inginerie electrica, No.35, 2011, ISSN 1842-4805, pp. 31-38.
- [11] J W. Kolar, H Ertl, Status of the Techniques of Three-phase Rectifier Systems with Low Effects on the Mains, 21st INTELEC, Copenhagen, Denmark, June 6-9, 1999.
- [12] M Xue, M He, Control of Unit Power Factor PWM Rectifier, Energy and Power Engineering, may 2013, pp. 121-124, doi:10.4236/epe.2013.54B023 Published Online July 2013 (<http://www.scirp.org/journal/epe>).
- [13] I Syed, MBS Reddy, KH Babu, Unity Power Factor Control by PWM Rectifier, IJRET, Volume: 02 Issue: 10 | Oct-2013, eISSN: 2319-1163 | pISSN: 2321-7308.
- [14] P Manikandan, SP Umayal, A Mariya Chithra Mary, M Ramachandran, Simulation And Hardware Analysis Of Three Phase PWM Rectifier With Power Factor Correction, IOSR Journal of Electrical and Electronics Engineering (IOSR-JEEE) e-ISSN: 2278-1676, p-ISSN: 2320-3331, Volume 8, Issue 1 (Nov. - Dec. 2013), pp 27-33.
- [15] Control Desk Experiment Guide for release 5.2, dSpace GmbH, 2006.